

Refractive Focusing by Interstellar Clouds and the Rapid Polarization Angle Swing in QSO 1150+812

Shan-Jie Qian¹, T. P. Krichbaum², Xi-Zhen Zhang¹, L. Fuhrmann², G. Cimò²,
A. Kraus², T. Beckert², S. Britzen³, A. Witzel² and J.A. Zensus²

¹ National Astronomical Observatories, Chinese Academy of Sciences, Beijing 100012;
rqsj@bao.ac.cn

² Max-Planck-Institut für Radioastronomie, Auf dem Hügel 69, 53121 Bonn, Germany

³ Max-Planck-Institut für Astronomie, Königstuhl 17, 69117 Heidelberg, Germany

Received 2005 January 8; accepted 2005 August 20

Abstract A very rapid polarization position angle swing of $\sim 180^\circ$ (with a time scale of ~ 6 hours) observed at 2 cm in QSO 1150+812 ($z = 1.25$) was reported by Kochenov & Gabuzda. This very rare event is difficult to explain. We found a possible interpretation in the framework of a source model consisting of three polarized components, in which two compact polarized components are nearly simultaneously occulted by an interstellar cloud, with consequent focusing-defocusing effects. A specific plasma-lens model is proposed which can reasonably fit the polarized flux density curve with results derived for the two lensed components. Some physical parameters of the plasma-lens and the source components are estimated. The two compact polarized components are estimated to have brightness temperatures of $\sim 6 \times 10^{12}$ K. Thus a bulk relativistic motion with a Lorentz factor less than 10 is required to meet the inverse-Compton limit.

Key words: radio continuum: galaxies – galaxies: compact – polarization – scattering – quasars: individual: 1150+812

1 INTRODUCTION

Intraday variability (IDV, hereafter) is a common phenomenon in flat-spectrum compact extragalactic radio sources (Wagner & Witzel 1995) and have been investigated intensively in recent years. In comparison with the original definition of IDV (Heeschen 1987; Witzel 1986), now the timescale of IDV has been extended in the direction of smaller scales to range from ~ 1 day to $\lesssim 1$ h. Correspondingly, the apparent brightness temperature ($T_{b,app}$) derived from light travel-time arguments now ranges from $\sim 10^{16}$ K to $\sim 10^{21}$ K, in excess of the inverse-Compton limit by a factor of $\sim 10^4$ – 10^9 . Therefore, it seems that we may encounter diverse IDV events with different properties and involving different mechanisms. In fact, the optical–radio correlated intraday variations with a timescale ~ 1 day ($T_{app,b} \sim 10^{17}$ K) observed in the BL Lac object 0716+714 (Quirrenbach et al. 1991) were attributed to an intrinsic origin (Wagner et al. 1996; Qian et al. 1996). This event not only showed a similar time structure of the optical- and radio-light curves (including a change of time scale from ~ 1 day to ~ 1 week), but also displayed a tight correlation between the variations in the optical intensity and the radio spectral index between 3.6 cm and 6 cm. Four successive

optical peaks were clearly seen to be correlated with the flattening of the radio spectrum. Thus this event may not be interpreted as an accidental coincidence of intrinsic optical variation with radio scintillation. More generally, Spada et al. (1999) have proposed that electron sheets propagating through relativistic conical shocks can explain the IDV observed in 0716+714. This model specifically showed the possibility that in some cases relativistic shocks with a Lorentz factor of ~ 10 can be used to interpret IDV of apparent brightness temperatures $T_{b,app}$ of $\sim 10^{17}$ K.

In contrast, the extremely rapid variations observed in 0405–385 (Kedziora et al. 1997) and J1815+385 (Dennet-Thorpe & de Bruyn 2000) have timescales less than one hour and apparent brightness temperatures as high as $\sim 10^{21}$ K. Refractive scintillation by interstellar medium has been suggested as the dominant mechanism for the observed variations both in intensity and polarization (e.g., Rickett et al. 2002). In the two sources the annual modulation of the scintillation time scales caused by the Earth motion was observed (e.g., Dennet-Thorpe & de Bruyn 2000), supporting the scintillation interpretation.

In the intermediate cases (for example in 0954+658 and 0917+624), where the derived apparent brightness temperatures are in the range of $\sim 10^{17}$ – 10^{18} K, the situation appears more complex. Both intrinsic mechanisms (Qian et al. 1991; Gopal-Krishna & Wiita 1992; Marscher 1992, 1996) and refractive scintillation (Rickett et al. 1995; Wambsganss et al. 1989; Simonetti 1991; Qian 1995a, 2001a) have been investigated. Qian et al. (1991) suggested that relativistic shocks propagating through magnetized plasma turbulence along the jet may explain these intraday variations. This kind of variations of intensity and polarization caused by relativistic shocks were simulated by Marscher et al. (1992), with a good agreement shown between the simulated and the observed variations. A further discussion on this kind of models was given by Marscher (1996). Gopal-Krishna & Wiita (1992) suggested that intraday variations could be explained in terms of relativistic thin shocks moving along slightly curved trajectories due to relativistic aberration effects.

In order to disclose the internal structure of IDV light curves observed in 0917+624, Qian et al. (2001a, 2001c) have compared the intraday polarization variations at 20 cm and 2–6 cm. On the basis of the observed fact that the variation of the polarized flux density at 20 cm was strictly proportional to that of the total flux density, they found that refractive scintillation is dominant at 20 cm. However, they separated some significant features in the 20 cm light curve of polarized flux density, which were shown to vary simultaneously with those at 2–6 cm. Such simultaneous broadband variations (from 2 cm to 20 cm) could be due to an intrinsic origin. It is worth pointing out that for 0917+624, the annual modulation of scintillation time scale predicted by Rickett et al. (2001), Jauncey & Macquart (2001) (and also see Qian & Zhang 2001b) was not confirmed in the recent monitoring observations by Fuhrmann et al. (2002a). On the basis of the VLBI observations, the change of the IDV time scale in 0917+624 between 1997 and 1999 observed by Kraus et al. (1999) may be interpreted to be due to changes in the source structure (Krichbaum et al. 2002).

The IDV source 0954+658, similar to 0716+714, was observed to show correlated optical–radio intraday variations (Wagner et al. 1993). However, Cimò et al. (2002) recently detected an extreme scattering event (ESE) with a time scale of ~ 1 day, which is much shorter than the timescales (1–2 months) of the ESEs observed by Fiedler et al. (1987, 1994) in this source. All these ESEs are explained in terms of refractive focusing by interstellar clouds. Recently, Fuhrmann et al. (2002b) detected a huge CO-molecular cloud in front of the source. These observations show that refractive focusing by discrete clouds may play a significant role in causing the intraday variations in the source. However, in addition to the intraday ESE which is highly wavelength dependent, simultaneous broadband variations (at least from 2.8 cm to 11 cm) were also observed. It is unclear whether these variations could also be interpreted by the refractive focusing processes.

It seems possible that in sources like 0954+658 and 0917+624, intraday variations are a mixed phenomenon of scintillation and intrinsic variations (e.g. Krichbaum et al. 2002).

VLBI polarization observations are important for the study of IDV sources, because usually variability of polarization (polarized flux density and polarization position angle) is more dramatic than that of total flux density (Qian et al. 1991), and IDV components can be recognized in VLBI polarization maps. The relationship between the variability of polarization and total flux density can provide significant information for the origin of these variations. For several IDV sources, including 0716+714, 0917+624, 2155–152 and 1150+812, VLBI polarization observations have been

carried out by Gabuzda et al. (1997, 2000a, 2000b, 2000c). They found that in a few cases significant polarization variations were observed, but without substantial changes in total flux density. They argued in favor of an intrinsic origin of these intraday polarization variations and indicated that there is mounting evidence that a substantial fraction of IDV includes an appreciable, or even dominant, intrinsic component. These polarization variations could be associated with changes in either the degree of polarization or the position angle. Shocks propagating through a helical field may represent one possible mechanism for producing rapid changes in polarization without substantial variations of intensity.

In addition, even for the cases of extremely rapid variations with timescales of $\lesssim 1$ h, scintillation could not explain all the observed properties of IDV. For example, for the source 0405–385, in the framework of scintillation interpretation, the brightness temperature was derived to be $\gtrsim 5 \times 10^{14}$ K (Kedziora et al. 1997; Jauncey et al. 2000). This implies that a bulk relativistic motion with a Lorentz factor of ~ 500 – 1000 would be required if relativistic effect is to be used to bring down the high brightness temperature to the inverse-Compton limit. Such Lorentz factors seem unreasonably high and coherent radiation mechanisms may be required.

From all these observational facts and theoretical arguments, it seems that both scintillation (normal scattering by a refractive screen and refractive focusing by clouds) and intrinsic mechanisms (relativistic effects and coherent radiation) should be further investigated in the study of radio intraday variations.

In this paper we will discuss the interpretation of the rapid polarization position angle swing of $\sim 180^\circ$ observed in QSO 1150+812 by Kochenov & Gabuzda (1999), and try to identify the relevant conditions.

2 RAPID POLARIZATION POSITION ANGLE SWING IN 1150+812

2.1 Introduction

For the study of IDV in extragalactic radio sources, rapid polarization position angle swings of $\sim 180^\circ$ with time scales of $\lesssim 1$ day may be of particular interest. Such continuous polarization position angle swings are a regular behaviour (to some extent), which should imply some kind of regularity in the responsible physical process. Thus their study may be useful to further understanding of the physics of IDV. Until now, two polarization angle swing events have been observed: one in 0917+624 (Quirrenbach et al. 1989) at 6 cm and the other in QSO 1150+812 (Kochenov & Gabuzda 1999) at 2 cm. Interestingly, the two events were observed at two epochs some 10 years apart by different observers in different sources, so the existence of intraday polarization angle swings of $\sim 180^\circ$ is firmly established. Both intrinsic and extrinsic (scintillation) mechanisms have been proposed to explain these swings.

Quirrenbach et al. (1989) suggested that the polarization angle swing event observed in 0917+624 might be caused by a relativistic shock propagating along the jet and illuminating a helical magnetic field. This is an ‘intraday version’ of the model proposed by Königl & Choudhuri (1985) to interpret polarization angle swing events with time scales of months or years observed in extragalactic radio sources. This interpretation is based on the relativistic effects when the transverse field component rotates. Qian et al. (1991, 2002) considered a two-component model, in which a relativistic shock propagates along the jet and the vector combination of its synchrotron radiation with the steady polarized component leads to the swing of resultant polarization angle. The main characteristic of the shock model is that both the degree and angle of polarization of the shock component are variable. This shock model can explain not only the polarization angle swing of $\sim 180^\circ$, but also the normal behaviour of intraday polarization variations (correlation and anti-correlation between the variability of intensity and polarized flux density), especially the transition between polarization angle swing and normal polarization variability. In this model the degree and angle of polarization of the shock component are required to vary only over a small range. Gopal-Krishna & Wiita (1992) suggested that the relationship between the polarized and total flux density observed in IDV sources (correlation and anti-correlation) could be explained by a relativistic thin shock moving along slightly curved trajectories. In their model the degree of polarization of the shock component changes due to relativistic aberration effects.

Rickett et al. (1995) proposed a scintillation model to explain the intraday variations of intensity and polarization observed in 0917+624. However, the event of polarization angle swing of $\sim 180^\circ$ observed in the source could not be interpreted and was suggested to be due to a low level of intrinsic activity. This suggestion implied that during the polarization angle swing intrinsic activity could temporarily dominate over scintillation. However, how this transition could happen and why the intrinsic variability could play its role only during the polarization angle swing (and not for the entire IDV event) remain to be clarified. The failure to explain the polarization angle swing of $\sim 180^\circ$ might have been regarded as a shortcoming of the scintillation model, which significantly restricts its application to intraday polarization variations. We point out that in the case of scintillation an individual component keeps its degree and angle of polarization constant while its intensity and polarized flux density fluctuate due to the refractive scattering. So two or more scintillating components could not vary in concert to produce a continuous polarization angle swing of $\sim 180^\circ$ through refractive scattering by a turbulent screen.

Simonetti (1991) suggested that the polarization position angle swing of $\sim 180^\circ$ observed in 0917+624 could be interpreted in terms of refractive focusing by an interstellar shock passing in front of the source. Two polarized components (designated A and B) were assumed in the source, having their polarizations approximately differing by 90° , but only one (component A) is affected by the shock. As the shock passes across the line of sight, the plasma of the pre-shock region first makes component A strongly focused, causing a rapid increase of its intensity (and polarized flux density). At this stage the polarization angle of the source will be close to that of component A. Then, when the plasma of the post-shock region propagates across the line of sight it makes component A defocused and causes a rapid decrease of its intensity (and polarized flux density). At this stage the source polarization angle approaches that of the component B. In this interpretation the variation of the polarization position angle is discontinuous, i.e., only a position angle ‘jump’ of $\sim 180^\circ$. Simonetti (1991) suggested that in order to explain the observed polarization position angles near the middle of the swing, some other mechanism (intrinsic or focusing by another cloud) is needed. Obviously this would raise questions similar to those mentioned above for the scintillation model. In addition, we should point out that the ‘jump’ of the total flux density which was predicted by the model to accompany the polarization position angle swing was not observed.

From the above description, we realize that to say that scintillation is a plausible mechanism for the observed intraday polarization variations, it is necessary for the model to interpret the intraday polarization position angle swing of $\sim 180^\circ$.

In this paper we will discuss such an interpretation for the polarization position angle swing of $\sim 180^\circ$ observed in QSO 1150+812.

2.2 The Swing Event of 1150+812

The event of rapid polarization position angle swing of $\sim 180^\circ$ observed at 2 cm in QSO 1150+812 (Kochenov & Gabuzda 1999) is shown in Figure 1.

From Figure 1 it can be seen that the swing event shows some interesting properties.

- (a) During the entire period of the observation (~ 24 hours) the variability index of total flux density is $\sim 1.5\%$ (the average flux density is 1.327Jy), i.e. the total flux density only varied by a very small amplitude. During the most rapid swing period (from ~ 20 h to ~ 25 h) the total flux density had a minimum with a flux drop of ~ 60 mJy with a timescale of ~ 1 h;
- (b) The variability index of the polarized flux density is $\sim 13\%$ (the average polarized flux density is 30.9 mJy), showing a larger amplitude of variability than that of the total flux density. However, during the most rapid swing period, the polarized flux density was almost kept at a constant level. For the five observational points (from ~ 20 h to 25 h), the average of the polarized flux density is 31.4 mJy with a standard deviation of 0.4 mJy;
- (c) The total flux density had another rapid drop at ~ 12 h, but the polarized flux density and the polarization position angle changed only a little;
- (d) At both ~ 19 h and ~ 25.8 h, the polarized flux densities are significantly higher than the averaged value, but the total flux densities only have a drop of ~ 20 mJy. These changes are also very rapid with time scales of ~ 1 –2 h;

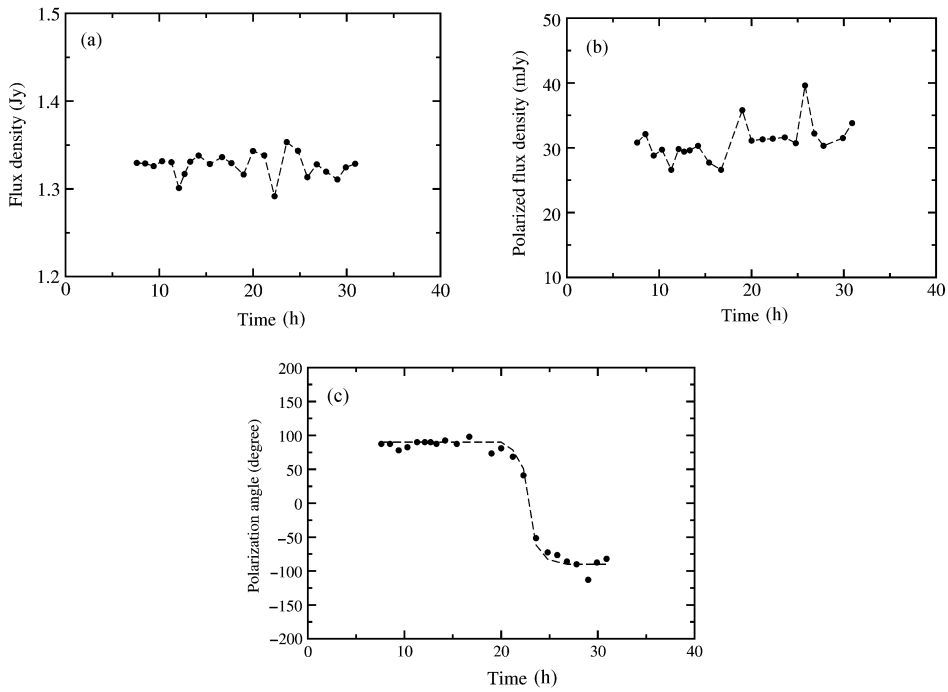


Fig. 1 A polarization position angle swing event observed in QSO 1150+812. Panels (a) to (c): the filled points are the observed data points of total flux density (Jy), polarized flux density (mJy) and polarization position angle reproduced from Kochenov & Gabuzda (1999). The dashed line in panel (c) represents the curve of polarization position angle, appropriately smoothed for the model-fitting (see text).

- (e) It is noted that the observed polarization angles fluctuate around 90° before the swing period and around -90° after the swing period, so the polarization angle swing is almost a complete half-circle.

The above properties of the polarization position angle swing seem difficult to explain, especially the relationship between the variations in the polarization (degree and angle) and in the total flux density. However, there are two observational facts that are useful for developing a new model.

First, the polarization position angle swing of $\sim 180^\circ$ was observed to be continuous, rather than a jump of the sort that would be explainable by the model of Simonetti (1991). This feature was also observed in the swing event of QSO 0917+624 (Qian et al. 1991; Quirrenbach et al. 2000): there were data-points near the middle of the swing, clearly showing the continuousness of the swing.

Secondly, for QSO 1150+812 we noticed that the most rapid swing occurs between the polarization angles of $\sim +50^\circ$ and $\sim -50^\circ$, the two nearly perpendicular to each other. The situation is similar in the swing event observed in QSO 0917+62 (Qian et al. 1991). As suggested by Simonetti (1991) we suppose that the two values given above may approximately represent the polarization angles of the polarized components in the core of the source. QSO 1150+812 has been mapped at 5GHz during the first Caltech-Jodrell Bank (CJ1) VLBI survey (Xu et al. 1995). The map shows a compact core-jet structure.

However, a two-component model cannot explain the observed polarization position angle swing, if the degree and angle of polarization of the two components remain constant, as in the case of interstellar scintillation (Rickett et al. 1995; Qian et al. 2002). We have considered a two-

component model, in which the two components vary in intensity but have constant, (both in degree and angle) nearly perpendicular polarizations. Through trial calculations we found that no matter how their polarized flux densities change, the vector combination of the two polarized components could not produce a continuous polarization position angle swing of $\sim 180^\circ$. In order to produce a continuous swing one more polarized component is needed.

3 A SPECIFIC MODEL

As we stated above, in order to explain a continuous polarization position angle swing of $\sim 180^\circ$ three polarized components are needed (models containing more than three variable polarized components are too complex to be considered). We have searched for possible ranges of the parameters of the components that will make a reasonable fit of the rapid swing event. In the following the three components are denoted as components 1, 2 and 3. The intensity, polarized flux density and polarization angle of the three components are designated by (I_1, p_1, χ_1) , (I_2, p_2, χ_2) and (I_3, p_3, χ_3) , respectively. Components 1 and 2 are assumed to be variable in polarized flux density, but their polarization angles remain constant. Component 3 is a steady component with its polarization angle substantially different from those of the two variable components.

3.1 Input Data-sets for Model-fitting

In the next section we will use the observational data to derive the parameters of the polarized jet components. Before doing so, we need to consider possible effects of the measuring errors of the observed quantities. Specifically, for example, we find that errors of about 10° – 20° in the measurements of the polarization angle could significantly affect the model-fitting results. Therefore, we will use a somewhat smoothed data set of polarization angle instead of the raw observations as input for our model-fitting in the next section. Specifically, for the time intervals (8h, 20h) and (26h, 31h) we will take the polarization angles to be equal to 90° and -90° , respectively; and for the swing period (21h, 25h) we will use a symmetrical curve to describe the angle swing. The input data set is shown by the dashed line in Figure 1c. It differs from the observed points by less than 20° .

In contrast, we will use the observed total and polarized flux densities (without any change) as input, since the effects of measuring error are smaller in these quantities than in the polarization angle. The two data sets are shown by the dashed lines in the (a) and (b) panels of Figure 1, respectively.

3.2 Parameters of the Model

On the basis of the data-sets given above, we can now construct a specific model for interpreting the polarization position angle swing of $\sim 180^\circ$ of 1150+812. For a three-component model the observed polarization should be the vector combination of the polarizations of the three components. We have the following equations for the Stokes parameters Q and U :

$$p_1 \cos 2\chi_1 + p_2 \cos 2\chi_2 + p_3 \cos 2\chi_3 = p \cos 2\chi, \quad (1)$$

$$p_1 \sin 2\chi_1 + p_2 \sin 2\chi_2 + p_3 \sin 2\chi_3 = p \sin 2\chi, \quad (2)$$

where $(p_1 \equiv p_1(t), \chi_1)$ and $(p_2 \equiv p_2(t), \chi_2)$ are the polarized flux density and position angle of the components 1 and 2, with p_1 and p_2 functions of time, and (p_3, χ_3) , those of the component 3. $(p \equiv p(t), \chi \equiv \chi(t))$ are the observed (known) polarized flux density and polarization angle. Equations (1) and (2) contain six unknown parameters, two of which are functions of time. So the equations are indeterminate and can not be solved generally. To start our procedure we have to choose some reasonable values for the four parameters $(\chi_1, \chi_2, p_3, \chi_3)$.

- First, as we have pointed out above, the observed polarization position angle swing occurred most rapidly from $\sim +50^\circ$ to $\sim -50^\circ$. As suggested by Simonetti et al. (1991), these angles possibly represent the polarization angles of the two jet components that are involved in the swing. They have their polarization angles approximately perpendicular to each other. So we

- specifically choose the polarization position angles of the components 2 and 3 to be $\chi_2=-40^\circ$ and $\chi_3=+45^\circ$, one of which might represent the jet direction in the core of the source. This choice is consistent with the VLBI polarization observations (e.g. Aarons 1999; Gabuzda et al. 2000d) that both longitudinal and transverse magnetic fields may exist in the cores of blazars.
- Secondly, in addition, the observation shows that outside the swing period ($t \lesssim 20$ h and $\gtrsim 25$ h), the observed polarization angle fluctuates around $\sim 90^\circ$, which is largely different from those of the components 2 and 3. This may imply that outside the swing period, the polarized flux density from the polarized component 2 approximately cancels that from the polarized component 3 and the observed polarization position angle may possibly represent that of the polarized component 1. Trial calculations for $\chi_1 = 80^\circ - 100^\circ$ showed that $\chi_1=95^\circ$ is an appropriate value;
 - Thirdly, we still need to choose a suitable value for p_3 . We note that during the swing period the observed polarized flux density is approximately equal to a constant (~ 30 mJy). This is the result of the vector combination of the three polarized components, two of which (components 1 and 2) are variable during the swing period. We found that p_3 should be less than ~ 40 mJy. Larger values of p_3 would produce large values of p_1 and p_2 , and the derived flux densities of the components 1 and 2 would be too large to fit the observed light curve of the total flux density. Trial calculations for $p_3=20-40$ mJy showed that $p_3=30$ mJy is an appropriate value.

The choice of the parameters described above is not unique, but based on some plausible arguments. The final results of the model-fitting discussed below would prove the choice to be appropriate.

3.3 Results of Model-fitting

Having chosen the values for the four parameters, and using the input data-sets of the polarized flux density and polarization angle chosen in Section 3.1, we can now solve Equations (1) and (2) for the variations of the polarized flux density of the component 1 and 2: $p_1(t)$ and $p_2(t)$. Given the four constants ($\chi_1, \chi_2, \chi_3, p_3$), Equations (1) and (2) give a unique solution for $p_1(t)$ and $p_2(t)$. The results are shown in Figure 2.

It can be seen that the light curves ($p_1(t)$ and $p_2(t)$) of the polarized flux density determined for the two components (1 and 2) are similar. Outside the polarization angle swing period, the two fluctuate with a very small amplitude, around their respective averages of 34.7 mJy and 24.3 mJy. They have a common feature: a deep minimum during the swing period, and for component 2 the light curve shows a prominent ‘peak’ at ~ 24.8 h following the minimum. We notice that for component 1 the minimum of the light curve is about 11.8 mJy, while for component 2 the corresponding

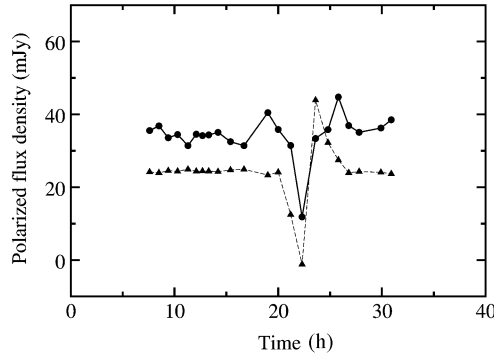


Fig. 2 Light curves of the polarized flux density determined for the two components (dots — $p_1(t)$ for component 1; triangles — $p_2(t)$ for component 2). The chosen values of the parameters are: $\chi_1=95^\circ$, $\chi_2=-40^\circ$, $\chi_3=+45^\circ$ and $p_3=30$ mJy. The input data-sets of the polarized flux density and the polarization position angle for the model-fitting are shown by the dashed lines in Figures 1b and 1c, respectively.

minimum is about -1.1 mJy. Although negative values of polarized flux density are not possible physically, this small negative value could be due to the oversimplification of the adopted model or due to the measuring errors in the observed polarized flux density which have not been taken into account (see Fig. 1b).

We point out that the light curves ($p_1(t)$, $p_2(t)$) derived above have profiles very like those of the extreme scattering events (ESE) discussed by Fiedler et al. (1987, 1994) and Clegg et al. (1996, 1998), but on a much shorter time scale of ~ 5 h. This implies that the polarization position angle swing of $\sim 180^\circ$ observed in QSO 1150+812 can be caused by a simultaneous ‘occultation’ of the two polarized components (1 and 2).

In the following section we will discuss a mechanism which can produce the light curves shown in Figure 2.

4 REFRACTIVE FOCUSING BY PLASMA-LENS

4.1 Introduction

We point out that the light curves of polarized flux density determined for the component 1 and 2 shown in Figure 2 are very similar to those observed in the so-called ESE, in which compact extragalactic radio sources are ‘occulted’ by interstellar clouds, but here the time scale (~ 5 h) is much shorter. Fiedler et al. found several ESEs through the monitoring observations with the Green Bank interferometer. At the low frequency (2.23 GHz), the light curves of intensity for these ESEs usually have time scales of weeks or months, with an extended minimum bracketed by two maxima (or bumps), but at the high frequency (8 GHz) there are multiple spikes. A ‘classical’ example is the event observed in QSO 0954+658. The properties of the ESEs were discussed in detail by Fiedler et al. (1987). They pointed out that these ESEs could not be due to some intrinsic origin and they interpreted them in terms of refractive scintillation: the extended minima observed at 2.23 GHz were interpreted as due to refractive defocusing by interstellar clouds, and the multiple spikes observed at 8 GHz, as due to refractive focusing or the formation of caustics (or ray crossing and multiple images). They estimated some parameters of the interstellar clouds (size, electron column density, distance to the observer, etc.) and of the compact source components (angular size, flux density). Romani et al. (1987) also proposed a detailed focusing–defocusing mechanism to explain the observed properties of ESEs. In addition to the ‘classical’ ESE observed in 0954+658, an ESE was observed in QSO 1741–038 by Clegg et al. (1996). The long-term multi-frequency light curves of flux density of this source were analysed by Qian et al. (1995b). They showed that the variations at the low frequencies are due to refractive scintillation while those at the higher frequencies (> 8 GHz) are intrinsic. The ESE was observed in 1992 (Clegg et al. 1996). At 2.23 GHz the time scale of the event was about 0.4 years. The behavior of the event in 1741–038 is different from that observed in 0954+658: the 8.1 GHz light curve did not show strong spikes, implying a weak refractive focusing. In 1741–038, therefore, even at 8 GHz both intrinsic variations and ESEs were observed.

Clegg et al. (1998) have proposed a Gaussian plasma-lens model to interpret the properties of the ESEs observed in both 0954+658 and 1741–038, on the basis of the geometric optics of refractive focusing process. They discussed the geometric optics of refraction of an extragalactic radio source by an interstellar plasma lens. The general properties are: around the axis of the plasma-lens, the defocusing of the source intensity forms an extended minimum in the light curve, and at both sides of the minimum the lens focusing forms sharp caustic spikes (if the source is very compact) or bumps (if the source is comparable to the lens in size). At higher frequencies caustic spikes can be formed even within the extended minimum. The properties of the lens and the compact source components can be estimated. Clegg et al. (1998) also pointed out that lens-grazing effects in a Gaussian lens model or a non-Gaussian plasma lens could explain the absence of the bumps in the light curve outside the minimum produced by the defocusing effects.

Since the light curves derived for the polarized components 1 and 2 during the polarization position angle swing are very similar to those observed in 0954+658 and 1741–038 at the low frequency 2.23 GHz, we will apply the plasma-lens model to interpret our results. Although the plasma-lens model can not well fit the observed light curves of 0954+658 and 1741–038 at the high frequency (8 GHz), especially with regard to the multiple sharp spikes, the fit at the low frequency (2.23 GHz) is good and we will use this model to interpret our results of 1150+812.

4.2 Plasma-lens Model

The one-dimensional Gaussian plasma-lens model proposed by Clegg et al. (1998) contains two independent dimensionless parameters α and β_s ,

$$\alpha = \left(\frac{\sqrt{\lambda D}}{a} \right)^2 \left(\frac{\lambda r_e N_0}{\pi} \right) \quad (3)$$

and

$$\beta_s = \theta_s / \theta_l. \quad (4)$$

Numerically,

$$\alpha = 3.8 \times 10^{-3} \left(\frac{\lambda}{\text{cm}} \right)^2 \left(\frac{N_0}{\text{cm}^{-3} \text{pc}} \right) \left(\frac{D}{\text{pc}} \right) \left(\frac{a}{\text{AU}} \right)^{-2}, \quad (5)$$

where D is the distance of the plasma-lens to the observer, λ the wavelength, and a the linear size of the plasma-lens. The distribution of column free-electron density (N_e) is assumed to have a Gaussian form: $N_e(x) = N_0 \exp[-(x/a)^2]$ (coordinate x indicates the position transverse to the line of sight) and N_0 is the peak column electron density, θ_s the angular size of the source component, θ_l the angular size of the lens as seen by the observer. It can be seen that the parameter α is a function of the wavelength, the free-electron column density through the lens, the lens-observer distance and the diameter of the lens transverse to the line of sight. The refractive properties of the lens are specified completely by the dimensionless parameter α . However, the pattern of ESE light curves of the source which is lensed by the plasma-lens depends on the dimensionless parameter α and the angular size of the source component relative to that of the lens as seen by the observer. The time interval Δt between the peaks (or bumps) is a measure of the time scale of the focusing events. It is related to the linear size of the lens and the relative transverse velocity v of the lens with respect to the observer (Clegg et al. 1998):

$$\Delta t \approx 4.3a/v. \quad (6)$$

4.3 Model-fitting

Following the theory of geometric optics of refractive focusing given by Clegg et al. (1998), the ray-path equation for an extended source is solved to obtain the model light curve. We assume that the source brightness distribution $B(\theta)$ has a Gaussian form ($-\theta_s/2 \leq \theta \leq \theta_s/2$):

$$B(\theta) \propto \exp \left[- \left(\frac{\theta}{\theta_s} \right)^2 \right]. \quad (7)$$

Each ray incident on the lens at position x is refracted by a certain angle and strikes at a position x' on the plane of the observer. The ray-path equation giving the relation is

$$u[1 + \alpha \exp(-u^2)] - (u' + \beta) = 0, \quad (8)$$

where $\beta = \theta/\theta_s$, $u = x/a$ and $u' = x'/a$. For each ray-path a gain factor is calculated to define the ray strength after the focusing and defocusing. In our case of weak scattering, no ray crossing (or multiple images) takes place, and for a point source there is only one ray striking at any position on the observer plane. So the model light curve is obtained by integrating the contributions from all the rays from the extended source.

We have used the plasma-lens model to make a fit to the light curves shown in Figure 2. We found that a plasma-lens model with $\alpha=2.0$ and $\beta_s=1.0$ can produce a reasonable fit to the light curves of both components 1 and 2. The results are shown in Figures 3 and 4.

The values of α and β_s imply that the swing event occurred in weak refractive scattering. The variations in the total and polarized flux densities are solely due to refractive focusing and defocusing: no caustics formed. According to the theory of focusing the minimum of the light curve is equal to $1/(1 + \alpha)$: 11.6 mJy for component 1 and 8.1 mJy for component 2.

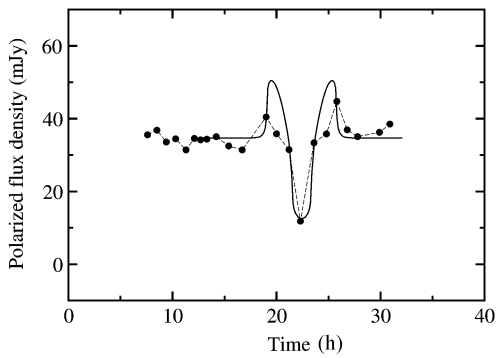


Fig. 3 Model-fitting of the light curve of the polarized component 1 with a plasma-lens model, $\alpha=2.0$ and $\beta_s=1.0$.

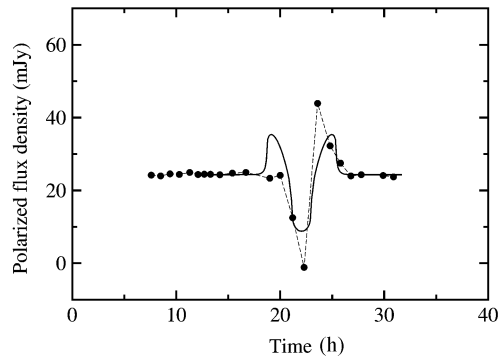


Fig. 4 Model-fitting of the light curve of the polarized component 2 with a plasma-lens model, $\alpha=2.0$ and $\beta_s=1.0$.

The angular sizes of the lensed components are similar to that of the lens, so the light curves are smoothed by the source sizes. The fittings in Figures 3 and 4 can be seen to be quite good, especially good for the minimum of component 1, and reasonably so for the minimum of component 2. However, the sampling of the observation was not dense enough to define the observed profiles for detailed comparison. The bumps predicted for component 1 by the model have no observed counterparts. For component 2 one of the bumps predicted by the model seems to have a counterpart which, however, occurred a little earlier.

Differences between the modelled and observed light curves usually appear when model-fitting is made, like in the cases of 0954+658 and 1471-038 (Clegg et al. 1998). They are usually interpreted to be due to substructures within the lens, to lens-grazing and/or to anisotropic lens profiles. Especially, the absence of the bumps predicted by a Gaussian plasma lens model may imply that the lens has a non-Gaussian profile (Clegg et al. 1998). This interpretation may be used to explain our model-fitting results, i.e. the distribution of the electron column density of the lens is not a Gaussian one. Similarly, for a few ESEs observed by Fiedler et al. (1994) and Clegg et al. (1988). Their light curves have a minimum associated with a single bump or a minimum without associated bumps. These events could be explained by interstellar shock models, in which the distribution of electron column density is non-Gaussian.

The modelled light curves show that the defocusing of the component 1 happened later than that of the component 2 by ~ 0.4 h. When component 2 was fully ‘occulted’, component 1 was also largely occulted, so there was almost simultaneous ‘occultation’ of the two components. The normal polarized flux densities of the components 1 and 2 are 34.7 mJy and 24.3 mJy, respectively.

On the basis of the modelled light curves of the polarized flux density, we can derive the light curves of the flux density for the two components, if the degrees of polarization of the components 1 and 2 are given. VLBI polarization observations with resolutions of $\gtrsim 0.1$ mas at centimeter wavelengths (for example, Gabuzda et al. 2000d) have shown that the observed degree of polarization is usually in the range $< 2\%$ for the core and up to 30% for the jet components, occasionally as high as $\sim 60\%$. In order to give a good fit to the observed total flux density curve (see Fig. 5b), a degree of polarization of 50% is assumed. This value is quite high, but might be still possible for such very rare swing events on scales of hours. As we will see below, for the polarization angle swing in 1150+812, the ‘occulted’ components (components 1 and 2) have angular sizes of $\sim 10\text{--}25\mu\text{as}$ and are located very close to each other in the ‘deep’ core of the source (within about $25\text{--}30\mu\text{as}$). Future space VLBI observations with resolutions of $\sim 3\text{--}5\mu\text{as}$ at centimeter wavelengths are required to check this supposition. In other words, adopting a high value of 50% for the degree of polarization of the source components is a necessary requirement for the proposed model-fitting. The available observations do not seem to completely rule out this possibility.

In Figure 5a is shown the derived light curve of the summed flux density of the two components. It has a minimum at ~ 22.3 h with a drop of flux density of ~ 100 mJy, corresponding to the

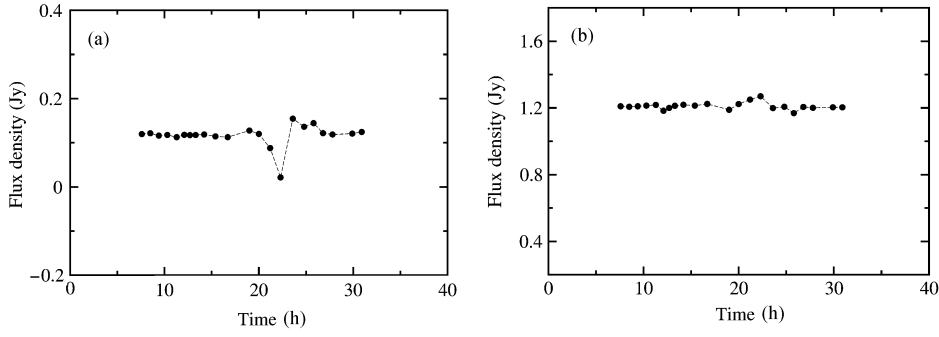


Fig. 5 (a) Light curves of the summed flux density of components 1 and 2; (b) the residual flux density obtained by subtracting the summed flux density from the total flux density.

occultation of the components during the swing period. There is a modest ‘bump’ following the minimum, which corresponds to the bump in the light curve of the polarized flux density of the component 2 (see Fig. 4). In Figure 5b is shown the residual flux density (total — summed). It can be seen that the residual does not vary much during the entire period of the observation. This indicates that the drop of the total flux density observed during the swing period is almost completely caused by the occultation of the component 1 and component 2. It also implies that within the fitting errors of the model (estimated to be $\sim 10\text{--}20\text{ mJy}$) the non-polarized components are not affected by the focusing-defocusing process. The reasonable fitting of the observed total flux density is an indication of the consistency of the model.

4.4 Estimation of Parameters

On the basis of the plasma-lens model some parameters of the source and the lens can be estimated. Since we do not know the value of the relative transverse speed between the lens and the observer, we shall use the following formulae:

$$\frac{a(\text{AU})}{v(\text{km s}^{-1})} \approx 5.6 \times 10^{-6} \Delta t(\text{h}), \quad (9)$$

$$\frac{\theta_s(\mu\text{as})}{v(\text{km s}^{-1})} \approx 5.6 \frac{\Delta t(\text{h})}{D(\text{pc})} \beta_s, \quad (10)$$

$$N_0(\text{cm}^{-3}\text{pc}) \approx 2.6 \times 10^{-10} \alpha \left(\frac{\lambda}{\text{cm}} \right)^{-2} \left(\frac{D}{\text{pc}} \right) \left(\frac{\theta_s}{\mu\text{as}} \right)^2 \beta_s^{-2}, \quad (11)$$

$$n_e(\text{cm}^{-3}) \approx 2.06 \times 10^5 \frac{N_0(\text{cm}^{-3}\text{pc})}{a(\text{AU})}, \quad (12)$$

$$M_l \approx 1.2 \times 10^{-17} \left(\frac{n_e}{\text{cm}^{-3}} \right) \left(\frac{a}{\text{AU}} \right), \quad (13)$$

where N_0 is the peak electron column density through the lens along the line of sight, n_e the electron density of the lens and M_l the mass of the lens.

We point out that the source 1150+812 is located in the direction to the Galactic Loop III and so we assume the plasma-lens is located in this Loop which may be a supernova remnant. The distance of the Loop has been estimated to be $\sim 130\text{ pc}$ (Fiedler et al. 1994). Thus if we take the velocity to be $30\text{--}100\text{ km s}^{-1}$, (note $\Delta t \simeq 5.9\text{ h}$), then we obtain the following estimates (in our

case the wavelength of observation is 2 cm):

$$\begin{aligned} a &= (1.0 - 3.3) \times 10^{-3} \text{ AU}, \\ \theta_s &= (6.8 - 23) \mu\text{as} \quad (\text{at } 2 \text{ cm}), \\ N_0 &= (0.9 - 10) \times 0^{-6} \text{ cm}^{-3} \text{ pc}, \\ n_e &= (1.8 - 6.2) \times 10^2 \text{ cm}^{-3}, \\ M_l &= (0.43 - 51) \times 10^{-23} M_\odot. \end{aligned}$$

These values show that the lensed polarized components are very compact and the lens is much smaller than those observed in ESEs. The electron density of the lens is much lower than those estimated for the ESEs observed by Fiedler et al. (1987) and Clegg et al. (1998), but very similar to those derived for the intraday ESE by Cimò (2002).

The brightness temperatures of the polarized components (1 and 2) can also be estimated.

$$T_b(\text{K}) = 2 \times 10^{15} (1+z) \left(\frac{S_{\text{obs}}}{\text{Jy}} \right) \left(\frac{\lambda_{\text{obs}}}{\text{cm}} \right)^2 \left(\frac{\theta_s}{\mu\text{as}} \right)^{-2}. \quad (14)$$

If we take $S_{\text{obs}}=0.060$ Jy (corresponding to a degree of polarization of 50% for a component with a polarized flux density of 30 mJy), and $\theta_s=14 \mu\text{as}$ (corresponding to $v=60 \text{ km s}^{-1}$), we obtain $T_b \simeq 5.5 \times 10^{12}$ K. Thus a relativistic motion with a Lorentz factor <10 is enough to bring the brightness temperature down to the inverse Compton limit. This upper limit is consistent with the VLBI measurements (Zensus 1997) for superluminal sources. However, if we take a smaller value for v (e.g. $<30 \text{ km s}^{-1}$), then the derived angular sizes of the lensed components would decrease and their brightness temperatures would increase correspondingly, leading to higher values of the Doppler factor.

Finally, we should emphasize that in our model the lensed components are very compact with angular sizes of only $\sim 20 \mu\text{as}$. They might be located in the VLBI core and so are closely to each other, and thus can be nearly simultaneously occulted by an interstellar cloud. For testing our model multi-frequency VLBI monitoring observations are required to find occultation events at different frequencies, like the one observed in the quasar 0528+134 (Pohl 1995). Moreover, associated variations in polarization should also be observed.

5 DISCUSSION

The polarization position angle swing of $\sim 180^\circ$ observed in QSO 1150+812 has been interpreted in terms of refractive focusing by an interstellar cloud. The results can be summarized as follows.

- The model proposed to explain the polarization position angle swing involves three polarized components: two lensed components (components 1 and 2) and one steady component (component 3). It has been shown that the polarization position angle swing observed in QSO 1150+812 is caused by the simultaneous occultation (defocusing) of the two polarized components (components 1 and 2) by an interstellar cloud (lens). Therefore, the polarization position angle swing event observed in 1150+812 indicates the importance of the focusing–defocusing effects of discrete clouds. Wambsganss et al. (1989) have shown that intraday variations of flux density can be caused by an assembly of clouds through refractive scintillation. In addition, Rickett et al. (1995) argued that refractive scintillation by a continuous interstellar medium can explain normal intraday variability of flux density and polarized flux density, but not polarization angle swings of 180° . Therefore, the interstellar scattering medium may consist of two constituents: a large-scale continuous medium and small scale discrete clouds. Combining the scattering effects of these two constituents, the general intraday variability and the regular behavior like polarization angle swing of $\sim 180^\circ$ can then be interpreted in a unified way, i.e., the rapid transition between a polarization position angle swing of $\sim 180^\circ$ and the normal polarization variability can be understood in the framework of the proposed model. Clegg et al. (1988) have suggested that expanding shock fronts can naturally create discrete plasma lens, while the general ISM is widely believed to have an extended, turbulent distribution of electron density fluctuation.

- In the case of 1150+812 the refractive focusing is a weak scattering process with $\alpha = 2.0$. The rounded minima of the light curves for both components 1 and 2 and the ‘bump’ for the component 2 have been reasonably well fitted by the proposed model.
- The polarization angles derived for the three polarized components imply that in the deep core of QSO 1150+812 magnetic fields with different orientations exist on scales of tens of μas (for example): longitudinal, transverse and oblique fields. Moreover, our model-fitting implies that on scales of tens of μas high degrees of polarization might occasionally occur in the source. An observational test would be helpful.
- The angular sizes derived for the lensed polarized components are in the range of $\sim 10\text{--}30\ \mu\text{as}$, and the corresponding brightness temperatures are in the range of $\sim (2\text{--}10)\times 10^{12}\ \text{K}$. Therefore, a relativistic bulk motion with a Lorentz factor $\lesssim 10$ may be enough to conform to the inverse-Compton limit.
- The cloud which causes the polarization position angle swing is extraordinarily small. It is only $(1\text{--}3)\times 10^{-3}\ \text{AU}$ in size. Its electron density is $\sim (2\text{--}6)\times 10^2\ \text{cm}^{-3}$.
- Although our model is only for explaining the polarization angle swing of $\sim 180^\circ$, the variations of the total and polarized flux density outside the swing (e.g., before $\sim 20\ \text{h}$) might have similar origin, i.e., they could be also due to focusing–defocusing by clouds of different sizes and structures, moving in front of the source and providing different focusing conditions, but not producing any regular pattern of variability like polarization position angle swings of 180° . Thus polarization angle swings and normal intraday variations, and the transition between these two states could be explained in a unified way.

Finally, we point out that the model proposed in this paper is not unique, leaving much room for the choice of alternative model parameters. Moreover, it is the only one of the available competing models for explaining polarization position angle swings. The model requires special conditions: there are three polarized components with special orientations and similar polarized flux densities, and two of them are simultaneously defocused by an interstellar cloud. Further observations (especially space VLBI polarization observations) are desirable to check these conditions and to find out whether two variable polarized components are, or only one is, involved in polarization angle swings. In the latter case intrinsic mechanisms may play a significant role (Qian et al. in preparation).

Acknowledgements We thank the anonymous referee for a critical reading of the manuscript and helpful comments. SJQ acknowledges the support from Max-Planck-Institut für Radioastronomie during a half year visit in 2002.

References

- Aarons S. E., 1999, In: BL Lac Phenomenon, ASP Conference series 159, eds. L.O. Takalo, A. Sillanpää, p.427
- Aller H. D., Aller M. F., Hughes P. A., 2002, In: Proceedings of the 6th European VLBI Network Symposium on new developments in VLBI Science and Technology, eds. E. Ros, R.W. Porcas, A.P. Lobanov, J.A. Zensus (MPIfR), p.111
- Cimò G., Beckert T., Krichbaum T. P. et al., 2002, Proc. Astron. Soc. Aust., 19, 10
- Clegg A. W., Chernoff D. F., Cordes J. M., 1988, In: Radio Wave Scattering in the Interstellar Medium, J. M. Cordes, B. J. Rickett, D.C. Backer, eds., New York: AIP, p.174
- Clegg A. W., Fey A. L., Fiedler R. L., 1996, ApJ, 457, L23
- Clegg A. W., Fey A. L., Lazio T. J. W., 1998, ApJ, 496, 253
- Dennett-Thorpe J., De Bruyn A. G., 2000, ApJ, 529, L65
- Fiedler R. L., Dennison B., Johnston K. J., Hewish A., 1987, Nature, 326, 675
- Fiedler R. L., Dennison B., Johnston K. J. et al., 1994, ApJ, 430, 581
- Fuhrmann L., Krichbaum T. P., Cimò G. et al., 2002a, Proc. Astron. Soc. Aust., 19, 64
- Fuhrmann L., Cimò G., Krichbaum T. P. et al., 2002b, In: E. Ros, R. W. Porcas, A. P. Lobanov et al., eds., Proceedings of the 6th European VLBI Network Symposium on new developments in VLBI Science and Technology, MPIfR, p.73

- Gabuzda D. C., Kochanov P. Yu., 1997, *Vistas in Astronomy*, 41, 219
- Gabuzda D. C., Kochanov P. Yu., Cawthorne T. V., Kollgaard R. I., 2000a, *MNRAS*, 313, 627
- Gabuzda D. C., Kochanov P. Yu., Cawthorne T. V., 2000b, *MNRAS*, 315, 229
- Gabuzda D. C., Kochanov P. Yu., Cawthorne T. V., 2000c, *MNRAS*, 319, 1125
- Gabuzda D. C., Pushkarev A. B., Cawthorne T. V., 2000d, *MNRAS*, 319, 1109
- Gopal-Krishna, Wiita P. J., 1992, *A&A*, 259, 109
- Heeschen D. S., Krichbaum T. P., Schalinski C. J., Witzel A., 1987, *AJ*, 94, 1493
- Jauncey D. L., Kedziora-Chudczer L., Lovell J. E. J et al., 2000, In: H. Hirabayashi, P. G. Edwards, D. W. Murphy, eds., *Astrophysical Phenomena Revealed by Space VLBI*, p.147
- Jauncey D. L., Macquart J.-P., 2001, *A&A*, 370, L9
- Kedziora-Chudczer L., Jauncey D. L., Wieringa M. H. et al., 1997, *ApJ*, 490, L9
- Kochanov P. Yu., Gabuzda D. C., 1999, In: L. O. Takalo, A. Sillanpää, eds., *BL Lac Phenomenon*, ASP Conference series 159, p.460
- Königl A., Choudhouri A. R., 1985, *ApJ*, 289, 188
- Kraus A., Witzel A., Krichbaum T. P. et al., 1999, *A&A*, 352, L107
- Krichbaum T. P., Kraus A., Fuhrmann L. et al., 2002, *Proc. Astron. Soc. Austr.*, 19, 14
- Marscher A. P., Gear W. K., Travis J. P., 1992, In: E. Valtaoja, M. Valtonen, eds., *Variability of Blazars*, Cambridge: Cambridge University Press, p.85
- Marscher A. P., 1996, In: H. R. Miller, J. R. Webb, J. C. Noble, *Blazar Continuum Variability*, ASP Conference series 110, p.248
- Pohl M., Reich W., Krichbaum T. P. et al., 1995, *A&A*, 303, 383
- Qian S. J., Quirrenbach A., Witzel A. et al., 1991, *A&A*, 241, 15
- Qian S. J., 1995a, *Chin. Astron. Astrophys.*, 19, 267
- Qian S. J., Britzen S., Witzel A. et al., 1995b, *A&A*, 295, 47
- Qian S. J., Li X. C., Wegner R. et al., 1996, *Chin. Astron. Astrophys.*, 20, 15
- Qian S. J., Witzel A., Kraus A. et al., 2001a, *A&A*, 367, 770
- Qian S. J., Zhang X. Z., 2001b, *ChJAA*, 1, 133
- Qian S. J., Kraus A., Krichbaum T. P. et al., 2001c, *Ap&SS*, 278, 119
- Qian S. J., Kraus A., Zhang X. Z. et al., 2002, *ChJAA*, 2, 325
- Quirrenbach A., Witzel A., Wagner S. et al., 1991, *ApJ*, 372, L71
- Quirrenbach A., Witzel A., Qian S. J. et al., 1989, *A&A*, 226, L1
- Quirrenbach A., Kraus A., Witzel A. et al., 2000, *A&AS*, 141, 221
- Rickett B. J., Quirrenbach A., Wegner R. et al., 1995, *A&A*, 293, 479
- Rickett B. J., Witzel A., Kraus A. et al., 2001, *ApJ*, 550, L11
- Rickett B., Kedziora-Chudczer L., Jauncey D. L., 2002, *Proc. Astron. Soc. Austr.*, 19, 106
- Romani R. W., Blandford R. D., Cordes J. M., 1987, *Nature*, 328, 324
- Simonetti J. H., 1991, *A&A*, 250, L1
- Spada M., Salvati M., Pacini F., 1999, In: L. O. Takalo, A. Sillanpää, eds., *BL Lac Phenomenon*, ASP Conference series 159, p.464
- Wagner S. J., Witzel A., Krichbaum T. P. et al., 1993, *A&A*, 271, 344
- Wagner S., Witzel A., 1995, *ARA&A*, 33, 163
- Wagner S. J., Witzel A., Heidt J. et al., 1996, *AJ*, 111, 2187
- Wambsgans J., Schneider P., Quirrenbach A. et al., 1989, *A&A*, 224, L9
- Witzel A., Heeschen D. S., Schalinski C. et al., 1986, *Mitt. Astron. Ges.*, 65, 239
- Xu W., Readhead A. C. S., Pearson T. J. et al., 1995, *ApJS*, 99, 297
- Zensus J. A., 1997, *ARA&A*, 35, 607